# BUCKLING ANALYSIS OF ANISOTROPIC CURVED PANELS AND SHELLS WITH VARIABLE CURVATURE

Navin Jaunky and Norman F. Knight, Jr.

Old Dominion University
Norfolk, VA 23529-0247

Damodar R. Ambur

NASA Langley Research Center
Hampton, VA 23681-0001

Presented at the 39th AIAA/ASME/ASCE/AHS/ASC
Structures, Structural Dymanics, and Material Conference

AIAA Paper 98-1772

Long Beach, California
April 20-23, 1998

# BUCKLING ANALYSIS OF ANISOTROPIC CURVED PANELS AND SHELLS WITH VARIABLE CURVATURE

Navin Jaunky* and Norman F. Knight, Jr.†
Old Dominion University
Norfolk, VA 23529-0247

Damodar R. Ambur‡
NASA Langley Research Center
Hampton, VA 23681-0001

## Abstract

A buckling formulation for anisotropic curved panels with variable curvature is presented in this paper. The variable curvature panel is assumed to consists of two or more panels of constant but different curvatures. Bezier functions are used as Ritz functions. Displacement ($C^0$), and slope ($C^1$) continuities between segments are imposed by manipulation of the Bezier control points. A first-order shear-deformation theory is used in the buckling formulation. Results obtained from the present formulation are compared with those from finite element simulations and are found to be in good agreement.

## Nomenclature

| | |
|---|---|
| $u_0$, $v_0$ | displacement along axial and transverse directions |
| $w$ | displacement along radial direction |
| $\phi_x$, $\phi_y$ | rotations of normals to middle surface or curvatures |
| $x$, $y$, $z$ | axial, circumferential, and normal coordinates |
| $f_i(n, \nu)$ | Bezier polynomial of order $n$ |
| $q_{ij}$ | Bezier control points |
| $\xi$, $\eta$ | non-dimensional coordinates |
| $L$ | length of segment |
| $S_I$ | width of segment $I$ |
| $R$ | Radius of curvature |

## Introduction

The use of composite materials for aircraft primary structures can result in significant benefits on aircraft performance and structural cost. Such applications of composite materials are expected to result in a 30-40 percent weight savings and a 10-30 percent cost reduction compared to conventional metallic structures. Shells with variable curvature are widely used for aircraft fuselage and wing components. The variable curvature configuration for these structures is due to aerodynamic and functional considerations. Hence the understanding of buckling behavior of composite shells with variable curvature is of importance for aerospace structural design.

The earliest work reported on the buckling analysis of shells with variable curvature was by Marguerre [1] in 1951. He expanded the curvature in a Fourier series with respect to the circumferential arc-length in order to more accurately represent the varying curvature of wing leading edge panels. His approach has been the basis for subsequent analyses of shells with varying curvature for both buckling ([2]-[4]) and vibration problems ([5]-[11]). In these References Marguerre's approach has been used for elliptical cylinders or panels since the variation of curvature ($1/R$) can be represented accurately by one term in the Fourier series. Reference [4] provides

*Postdoctoral Research Associate, Department of Aerospace Engineering. Member AIAA.

†Professor, Department of Aerospace Engineering. Associate Fellow AIAA.

‡Assistant Head, Structural Mechanics Branch. Associate Fellow AIAA.

an excellent review for buckling and vibration of shells and panels with variable curvature.

In addition to elliptical cylinders or panels, shells with varying curvature such as isotropic conical ([12, 13]) and torispherical shells ([13]) have been analyzed for free vibration. Irie et al. [12] used the transfer matrix technique to obtain natural frequencies of truncated conical shells. According to Reference [12], the advantage of the transfer matrix technique is its simplicity compared to other methods which require considerable analytical effort and computational time. A review of the literature for conical shell shell buckling is provided in Reference [12]. Singh ([13]) used a segment approach where a series of circular arc segments tangential to each other at the segment interface juncture is used to model the shell with varying curvature (e.g., conical and torispherical shell) without any approximation in geometry. Trigonometric and quintic Bezier polynomials are used to represent displacement fields in each arc segment. Smooth deformed surface of the shell are obtained by imposing $C^0$ and $C^1$ continuities at the juncture of two adjacent shell segments by using the properties of the Bezier control points. Also boundary conditions are applied by simple manipulation of the Bezier control points. Bezier polynomials have been used in a segment approach for the free vibration of isotropic elliptic cylinders ([14]), composite elliptic cylinders ([15, 16]), and a laminated conical shell ([16]). A first-order shear-deformation theory has been used in References [15] and [16]. Detailed reviews of the free vibration of shells with variable curvature are discussed in References [13]-[16]. The method presented in References [13]-[16] can be applied to different shell geometries, shells with anisotropic material properties, and shells with arbitrary boundary conditions. In addition, the method can incorporate first-order shear-deformation theory or classical laminated plate theory and is computationally efficient.

The present analysis method for buckling of anisotropic shells with variable curvature uses a segment approach where displacement fields within each segment are represented by Bezier polynomials and a first-order shear-deformation theory is used. In general, segments can be used in both axial and circumferential directions, however the present implementation considers only segments in the circumferential direction. Continuity of displacement at the junctures of adjacent segments are imposed using $C^0$ and $C^1$ conditions obtained from the properties of the Bezier control points ([14]). The shell with variable curvature is assumed to consist of two or more curved panels of constant curvature which is representative of fuselage or wing structures.

The present paper summarizes the analysis approach. Two structure cases with curvature are analyzed to demonstrate the capabilities of the present analysis approach. Result from the present analysis are compared with those obtained from finite element analyses.

## Analytical Approach

The coordinate system and the displacement directions for a noncircular shell is shown in Figure 1. Any point in the wall of the shell is specified by means of curvilinear coordinate system $x$, $y$ and $z$, where $x$ is the axial coordinate fixed to mid-surface, $y$ is the circumferential coordinate which follows the median line of the transverse cross section, and $z$ is the radial coordinate normal to both $x$ and $y$. The noncircular shell is assumed to consist of two or more segments in the circumferential direction each of constant radius. The normal and tangent of the two segments at a juncture are equal as shown in Figure 1, where $\vec{n}_1 = \vec{n}_2$ and $\vec{t}_1 = \vec{t}_2$.

Bezier polynomials are used in the axial and circumferential directions to represent the displacement fields. The Bezier polynomial is given by

$$f_i(n,\nu) = \frac{n!}{(i-1)!\,(n-i+1)!}\,\nu^{i-1}\,(\nu-1)^{n-i+1} \tag{1}$$

where $n$ denotes the order of the polynomial and $0 \le \nu \le 1$. For a Bezier polynomial of order $n$, there are $(n+1)$ control points. Any point on the surface of the segment is given by a parametric function of the form

$$P_{rs}(\xi,\eta) = \sum_{r=1}^{X}\sum_{s=1}^{Y} f_r(\xi) f_s(\eta) q_{rs} \tag{2}$$

where the coordinates $\xi$ and $\eta$ are defined as

$$\begin{aligned} \xi &= x \,/\, L \\ \eta &= (y - y_i) \,/\, (y_{i+1} - y_i) \end{aligned} \tag{3}$$

with $0 \le \xi, \eta \le 1$, $X$ and $Y$ are the number of control points in the axial and circumferential direction respectively, and $q_{rs}$ are the Bezier control points or coefficients. The displacement vector can be written as

$$[u_0\ v_0\ w\ \phi_x\ \phi_y]_j^T =$$

$$\begin{bmatrix} P_{rs} & 0 & 0 & 0 & 0 \\ 0 & P_{rs} & 0 & 0 & 0 \\ 0 & 0 & P_{rs} & 0 & 0 \\ 0 & 0 & 0 & P_{rs} & 0 \\ 0 & 0 & 0 & 0 & P_{rs} \end{bmatrix}_j \begin{Bmatrix} q_{1rs} \\ q_{2rs} \\ q_{3rs} \\ q_{4rs} \\ q_{5rs} \end{Bmatrix}_j \quad (4)$$

where $u_0$ and $v_0$ are the axial and transverse membrane displacements, respectively, $w$ is the normal displacement and $\phi_x$ and $\phi_y$ are the curvatures. Subscript $j = 1, 2, 3, \ldots (XY)$. The control points for each degree of freedom can be used to impose boundary conditions on each degree of freedom on each segment.

Continuity of displacement functions along segment junctures are obtained by using the relations between control points of the adjacent segment based on $C^0$ and $C^1$ continuities. Figure 2 shows two adjacent segments and the control points that are involved in the $C^0$ and $C^1$ continuities for the case of eleven control points in the axial direction and six control points in the transverse directions, i.e., $X = 11$ and $Y = 6$. In the $I^{th}$ segment, control points $q_{k6}$ and $q_{k5}$ are related to control points $q_{i1}$ and $q_{i2}$ of the $(I+1)^{th}$ segment, where $i,\ k = 1,2,3,4,5,6$ according to

$$\begin{aligned} q_{6k} &= q_{1i} \\ q_{6k} &= \frac{S_I\ q_{5k} + S_{I+1}\ q_{2i}}{S_I + S_{I+1}} \end{aligned} \quad (5)$$

where $S_I$ and $S_{I+1}$ are the width of the $I^{th}$ and $(I+1)^{th}$ segment, respectively. Using these conditions the unknowns $q_{1i}$ and $q_{2i}$ are expressed in terms of $q_{5k}$ and $q_{6k}$, which are slaved to the master control points $q_{1i}$ and $q_{2i}$.

Since the buckling analysis involves first-order shear-deformation, only $C^0$ continuity is required in the variational formulation. However the advantage of also imposing $C^1$ continuity is not only to obtain a more accurate analysis but also to reduce the size of the stiffness and geometric stiffness matrices when a larger number of segments are used to represent the shell that is being analyzed. Table 1 shows the size of the matrices with the number of segments for different conditions of continuities when $X = 11$ and $Y = 6$. If the segments are joined to approximate a shell, the size of the matrices are less than that for a panel. The size of the stiffness and geometric stiffness matrices after assembly is given by

$$ISIZE = 5 \times X \times Y \times NSEG - 110 \times MJOIN \quad (6)$$

for $C^0$ and $C^1$ continuities, where $ISIZE$ is the matrix size, $NSEG$ is the number of segments, and $MJOIN = NSEG - 1$ for a panel and $MJOIN = NSEG$ for a shell, i.e., $MJOIN$ is the number of junctures.

The linear stiffness matrices are derived from the strain energy which is given by

$$U = \frac{1}{2}\int_A \{\epsilon\}^T \begin{bmatrix} A_{ij} & B_{ij} & 0 \\ B_{ij} & D_{ij} & 0 \\ 0 & 0 & C_{pq} \end{bmatrix} \{\epsilon\} dA \quad (7)$$

where $A_{ij}$ is the extensional stiffness coefficient matrix, $B_{ij}$ is the coupling stiffness coefficient matrix, $D_{ij}$ is the bending stiffness coefficient matrix and $C_{pq}$ is the transverse shear stiffness coefficient matrix. The strain vector is $\{\epsilon\}$ and

$$\{\epsilon\}^T = \{\epsilon_x^0\ \epsilon_y^0\ \gamma_{xy}^0\ \kappa_x\ \kappa_y\ \kappa_{xy}\ \gamma_{xz}\ \gamma_{yz}\}^T \quad (8)$$

The strain displacement relations are

$$\begin{aligned} \epsilon_x^0 &= \frac{\partial u_0}{\partial x} \\ \epsilon_y^0 &= \frac{\partial v_0}{\partial y} + \frac{w_0}{R} \\ \gamma_{xy}^0 &= \frac{\partial u_0}{\partial y} + \frac{\partial v_0}{\partial x} \\ \kappa_x &= \frac{\partial \phi_x}{\partial x} \\ \kappa_y &= \frac{\partial \phi_y}{\partial y} \\ \kappa_{xy} &= \frac{\partial \phi_x}{\partial y} + \frac{\partial \phi_y}{\partial x} + \frac{C_2}{2R}\left(\frac{\partial v_0}{\partial x} - \frac{\partial u_0}{\partial y}\right) \\ \gamma_{xz}^0 &= \phi_x + \frac{\partial w_0}{\partial x} \\ \gamma_{yz}^0 &= \phi_y + \frac{\partial w_0}{\partial y} - C_1\frac{v_0}{R} \end{aligned} \quad (9)$$

Here $C_1$ and $C_2$ are "tracer" coefficients used to implement different strain-displacement relations or shell theories. Accordingly when $C_1 = C_2 = 1$, the first approximation of Sanders-Koiter shell theory [17, 18] is obtained and when $C_1 = 1$, $C_2 = 0$, Love's shell theory [19] including transverse shear deformations is obtained. Finally, when $C_1 = 0$ and $C_2 = 0$, Donnell's shell theory [20] including transverse shear deformation is obtained.

The geometric stiffness matrix is derived from the work done, ($W_d$), by the applied prebuckling loading and is

$$W_d = \int_A ( \overline{N}_x \epsilon_{xNL} + \overline{N}_y \epsilon_{yNL} + \overline{N}_{xy} \gamma_{xyNL} ) dA \quad (10)$$

where the nonlinear strain components are

$$\begin{aligned} (\epsilon_x)_{NL} &= \frac{1}{2}(v_{0,x}^2 + w_{,x}^2) \\ (\epsilon_y)_{NL} &= \frac{1}{2}(u_{0,y}^2 + (w_{,y} - \frac{v_0}{R})^2) \\ (\gamma_{xy})_{NL} &= -u_{0,y}(v_{0,y} + \frac{w}{R}) - v_{0,x} u_{0,x} \\ &\quad + w_{,x}(w_{,y} - \frac{v_0}{R}) \end{aligned} \quad (11)$$

In the present analysis the applied prebuckling loading is prescribed as a uniform in-plane stress state. The linear stiffness and geometric stiffness matrices are developed using analytical integration rather than numerical integration for computational efficiency. Finally, an eigenvalue problem is solved for determining the critical buckling load.

## Numerical Results

Results are presented for a composite cylindrical panel subjected axial compression and a composite wing leading-edge panel subjected to combined axial compression and shear. Sanders-Koiter ([17, 18]) shell theory is used in these studies. Buckling loads from the present analysis are compared with those obtained from the STAGS ([21]) finite element code. The STAGS finite element model consists of the 410 element and curved surfaces are approximated as an assembly of flat surfaces. The nominal ply mechanical properties for the composite material used are: $E_{11}$ = 13.75 Msi; $E_{22}$ = 1.03 Msi; $G_{12}$=$G_{13}$=$G_{23}$ = 0.420 Msi and $\nu_{12}$ = 0.250, and the laminate ply stacking sequence is $[\pm 45/0/90/\pm 45]_s$ with equal ply thickness for different laminate thickness.

### Cylindrical Panel

The first structure analyzed is a semicircular ($\alpha$ = 180°) cylindrical panel 22.0-in. long, and with a radius of 40.0 inches, as shown in Figure 3. The simply-support boundary conditions are also shown in Figure 3. The cylindrical panel is modeled as five curved segments in the present analysis while the STAGS finite element modeled consists of 20 and 40 elements in the axial and transverse direction respectively. Table 2 shows the results for the curved panel subjected to axial compression load.

The results in Table 2 suggest that for $t$ = 0.072 in. the present analysis result is 4.3 percent greater than the STAGS result while for $t$ = 0.144 in. and 0.216 in. the STAGS analysis results is 1.4 percent below that of the present analysis. The difference between results is due to using the 410 shell element of STAGS which do not include transverse shear deformation. The STAGS results are above that of the present analysis for $t$ = 0.144 in. and 0.216 in. since these two panels are thicker and transverse shear deformation effects are significant. The buckling mode shape for the curved panel obtained from STAGS analysis results is shown in Figure 4.

### Wing Leading-Edge Panel

The wing leading-edge panel is shown in Figure 5. It consists of three curved segments of radii 50.0 in., 6.136 in., and 50.0 in., respectively. The boundary conditions of the panel is shown in Figure 5 and correspond to classical simply support conditions. Each ply of the laminate is 0.006-in. thick. Using the present analysis, the wing leading edge was modeled as combination of two segments for the 50.0-in. radius section and one segment for the 6.136-in. radius section. The STAGS finite element model consists of the 410 shell element and 30×30 elements in each curved segment, and the formulation of the 410 element is based on the classical laminated plate theory. Table 2 shows the results obtained from the present analysis and those from STAGS for some selected combined load cases and Figure 6 shows the buckling load interaction curve between axial compression and positive shear loading.

The results from the present analyses are about 4.0 percent above those of STAGS except for the case of negative shear loading where the result from the present analysis is 6.4 percent above that of STAGS. Better agreement can be obtained from the present method by using more control points in the axial direction. However this will lead to more computational effort and the present percentage difference between STAGS and results from the present analyses is considered acceptable for a preliminary design. The buckling mode shape for the wing leading

edge obtained from STAGS analysis results are shown in Figure 7, 8 and 9 for axial compression, and positive and negative shear, respectively. The shell deformation is mostly in the 50.0-in. radius curved segments. For the case of positive shear, the shell deformation is mostly in one of the 50.0-in. radius curved segment.

## Concluding Remarks

A formulation has been developed for buckling of anisotropic laminated shells with variable curvature. The variable curvature is approximated by two or more segment of constant but different curvatures. Bezier polynomials are used as Ritz functions in the structural axial and transverse directions. Displacement ($C^0$) and slope ($C^1$) continuity are imposed between segments. Results obtained from the formulation are validated using finite element simulations. Buckling loads obtained from finite element solutions are determined to be four percent lower than those of the present analysis.

## Acknowledgement

The work of the first two authors was supported by NASA Grant NAG-1-1588 and is gratefully acknowledged.

# References

[1] K. Marguerre, "Stability of the Cylindrical Shell of Variable Curvature," NASA TM 1302, 1951.

[2] Chen, Y. N., and Kempner J., "Large Deflection of an Axially Compressed Oval Cylindrical Shell," Proceeding of $9^{th}$ International Congress on Applied Mechanics," Munich, Germany, 1964, Springer-Verlag, Berlin, pp. 299-305, 1965.

[3] Sheinman, I. and Frier, M., "Buckling Analysis of Laminated Cylindrical Shells with Arbitrary Noncircular Cross Section," *AIAA Journal*, Vol. 32, No. 3, March 1994, pp. 648-661.

[1] Carol A. Meyers, "An Analytical and Experimental Investigation of Elliptical Composite Cylinders," Virginia Polytechnic Institute and State University, Ph. D. dissertation in Engineering Science and Mechanics, April 1996.

[5] Boyd, D. E., "Analysis of Open Non-circular Cylindrical Shells," *AIAA Journal*, Vol. 7, No. 3, 1969, pp. 563-565.

[6] Kurt, C. E., and Boyd, D. E., "Free Vibration of Non-circular Cylindrical Shell Segments," *AIAA Journal*, Vol. 9, No. 2, 1971, pp. 239-244.

[7] Culberson, L. D., and Boyd, D. E., "Free Vibrations of Freely Supported Oval Cylinders," *AIAA Journal*, Vol. 9, No. 8, 1971, pp. 1474-1480.

[8] Elsbernd, G. F., and Leissa, A. W., "The Vibrations of Son-circular Shells with Initial Stresses," *Journal of Sound and Vibration*, Vol. 29, No. 3, 1973, pp. 309-329.

[9] Chen, Y. N., and Kempner, J., "Modal Method for Free Vibration of Oval Cylindrical Shells with Simply Supported or Clamped Ends," *ASME Journal of Applied Mechanics*, Vol. 45, No. 1, 1978, pp. 142-148.

[10] Koumousis, V. K., and Armenakas, A. E., "Free Vibration of Non-circular Panels with Simply Supported Curved Edges," *ASCE Journal of Engineering Mechanics*, Vol. 110, No. 5, 1984, pp. 810-827.

[11] Koumousis, V. K., and Armenakas, A. E., "Free Vibration of Simply Supported Cylindrical Shells," *AIAA Journal*, Vol. 21, No. 7, 1983, pp. 1017-1027.

[12] Irie, T., Yamada, G., and Kaneko, Y., "Free Vibration of of a Conical Shell with Variable Thickness," *Journal of Sound and Vibration*, Vol. 82, No. 1, 1982, pp. 83-94.

[13] Singh, A. V., "On Vibrations of Shells of Revolution Using Bezier Polynomials," *ASME Journal of Pressure Vessel Technology*, Vol. 113, November 1991, pp. 579-584

[14] Kumar, V., and Singh, A. V., "Vibration Analysis of Non-circular Cylindrical Shells Using Bezier Functions," *Journal of Sound and Vibration*, Vol. 161, No. 2, 1993, pp. 333-354.

[15] Kumar, V., and Singh, A. V., "Vibration of Composite Non-circular Cylindrical Shells," *ASME Journal of Vibration and Acoustics*, Vol. 117, October 1995, pp. 470-476.

[16] Kumar, V., and Singh, A. V., "Vibration of Fiber-Reinforced Laminated Deep Shells," *ASME Journal of Pressure Vessel Technology*, Vol. 118, November 1996, pp. 407-414.

[17] Sanders, J. L. Jr., "An Improved First Approximation Theory for Thin Shells," NASA Report R-24, 1959.

[18] Koiter, W. T., "A Consistent First Approximation in General Theory of Thin Elastic Shells," The Theory of Thin Elastic Shells, Proceedings IUTAM Symposium, Delft, 1959, pp. 12-33, 1960, Amsterdam, the Netherlands, North-Holland Publishing Company.

[19] Love, A. E. H., A Treatise on the Mathematical Theory of Elasticity, 4th edition, New York, Dover Publication, 1927.

[20] Loo, T. T., "An Extension of Donnell's Equation for Circular Cylindrical Shell," *Journal of Aeronautical Sciences*, Vol. 24, 1957, pp. 390-391.

[21] Brogan, F. A., Rankin, C. C., Cabiness, H. D., and William, A. L., "STAGS User's Manual," Lockheed Martin Missiles & Space Company Inc., Report LMMSC P032594, Version 2.3, 1996.

Table 1 Size of stiffness matrices for panel and shell for increasing number of segments.

| *NSEG* | *ISIZE* (Panel) $[C^0]$ | *ISIZE* (Panel) $[C^0, C^1]$ | *ISIZE* (shell) $[C^0, C^1]$ |
|---|---|---|---|
| 1 | 330 | 330 | - |
| 2 | 605 | 550 | 440 |
| 3 | 880 | 770 | 660 |
| 4 | 1155 | 990 | 880 |
| 5 | 1430 | 1210 | 1100 |
| 6 | 1705 | 1430 | 1320 |

Table 2 Comparison of buckling loads results for composite curved panel.

| Thickness $t$ (in.) | STAGS (lbs/in.) | Present analysis (lbs/in.) |
|---|---|---|
| 0.072 | 374.55 | 390.68 |
| 0.144 | 1481.08 | 1459.45 |
| 0.216 | 3328.25 | 3278.86 |

Table 3 Comparison of buckling loads results for wing-leading edge panel.

| Loading condition $N_x$ | Loading condition $N_{xy}$ | STAGS (lbs/in.) | Present analysis (lbs/in.) |
|---|---|---|---|
| 1.0 | 0.0 | 304.67 | 317.03 |
| 1.0 | 0.4 | 194.48 | 202.57 |
| 1.0 | 1.0 | 106.68 | 110.90 |
| 0.4 | 1.0 | 124.39 | 129.53 |
| 0.0 | 1.0 | -117.73 | -125.37 |
| 0.0 | 1.0 | 139.31 | 145.55 |

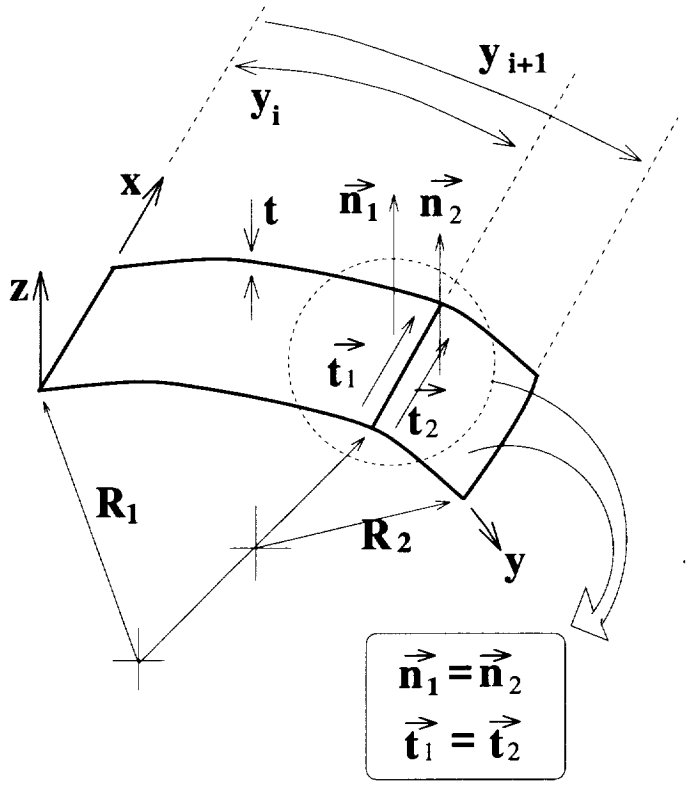


Figure 1: Coordinate system and geometry of shell with variable curvature.

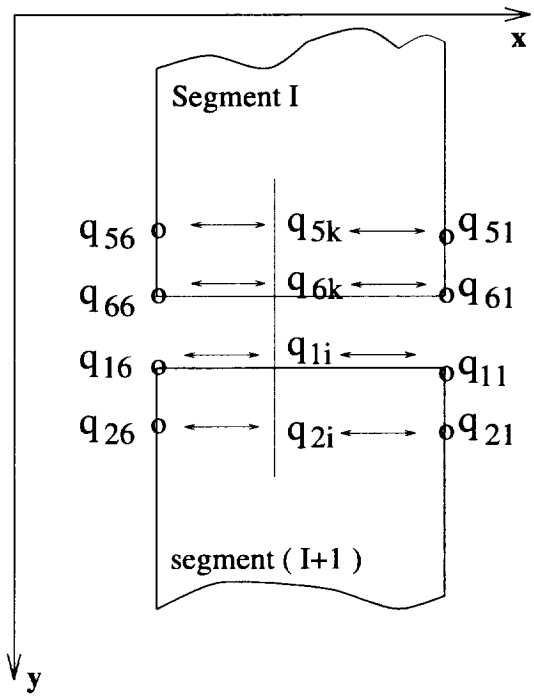


Figure 2: Control points for joining shell segments.

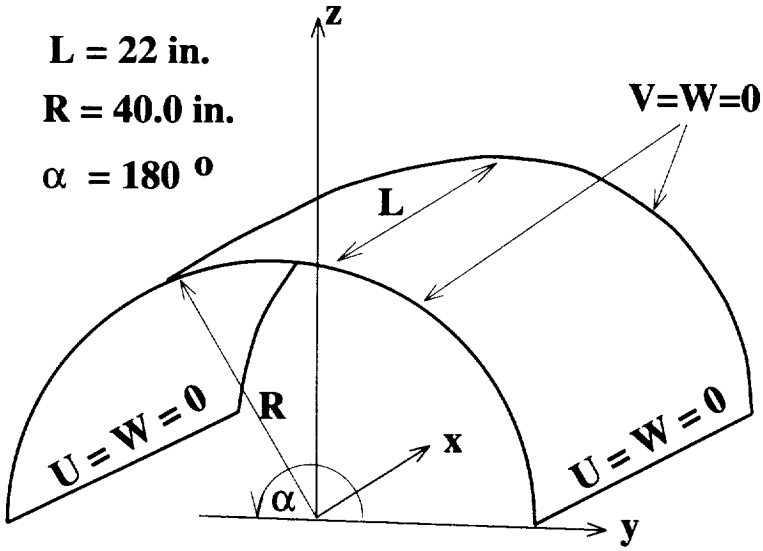


Figure 3: Geometry and boundary conditions of curved composite panel.

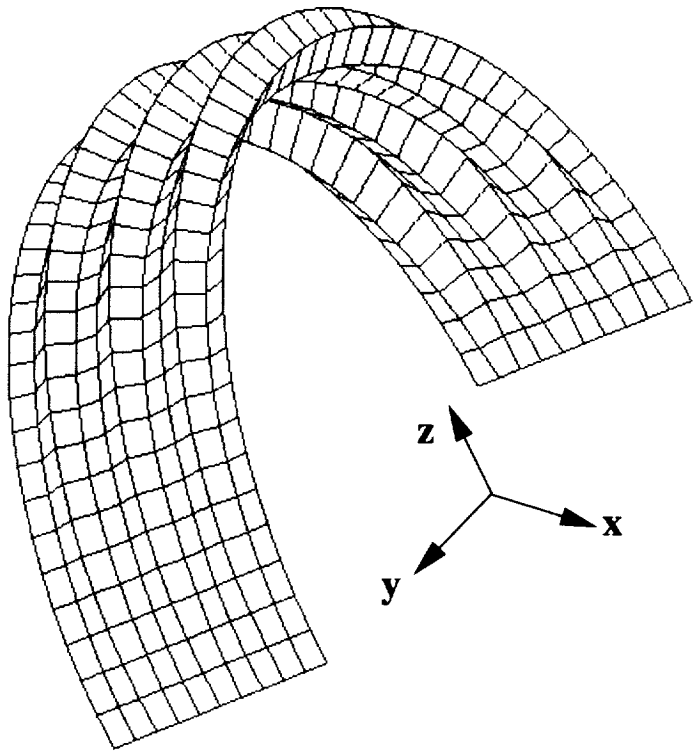


Figure 4: Buckling mode shape for curved composite panel.

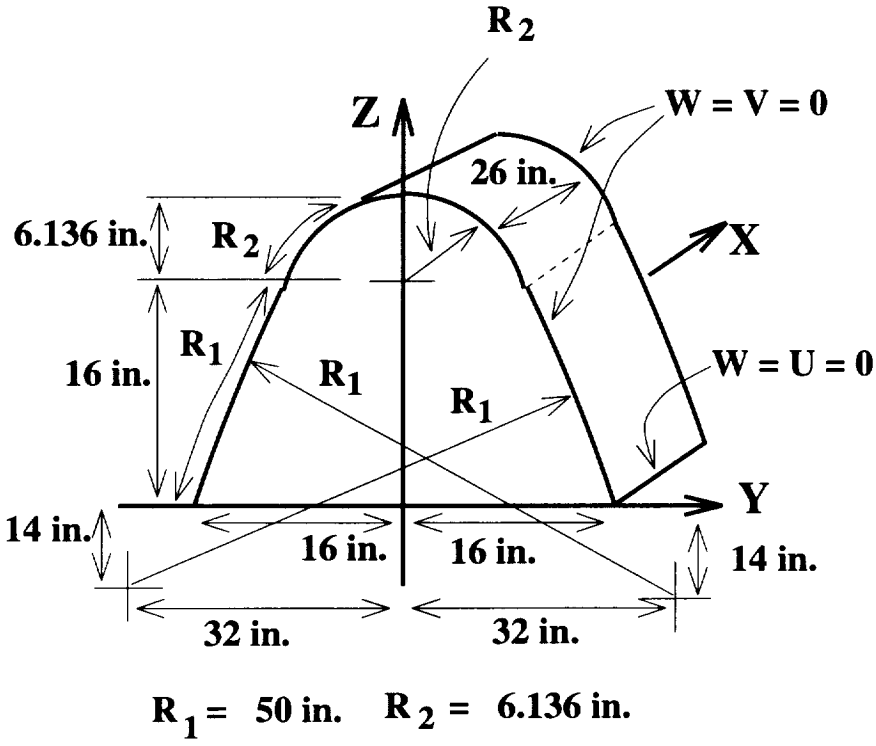


Figure 5: Geometry and dimensions of composite wing leading-edge panel.

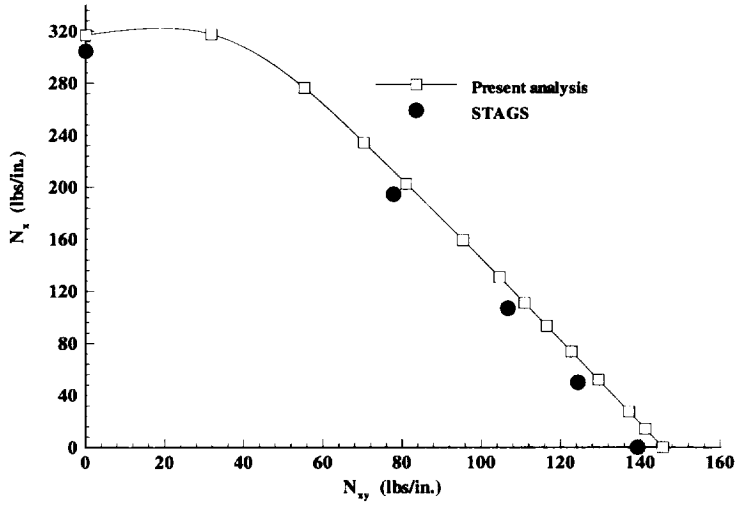


Figure 6: Buckling load interaction curve for the composite wing-leading edge panel.

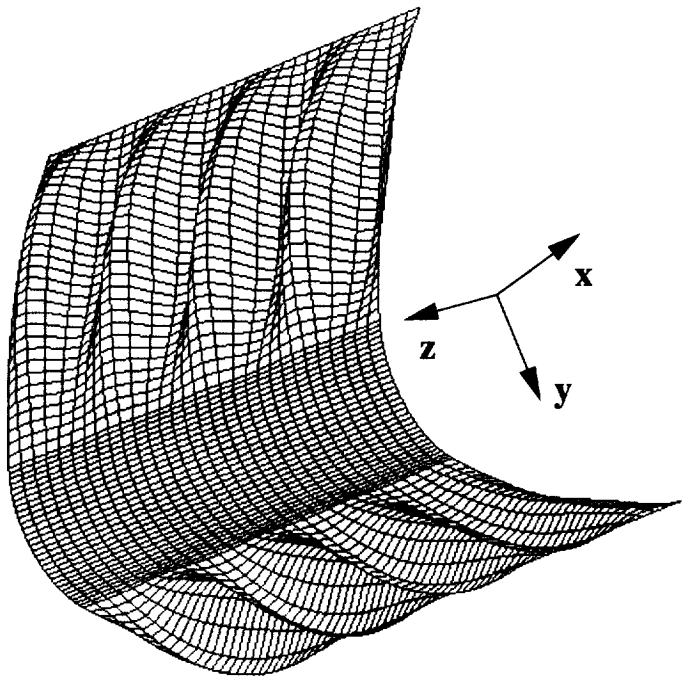


Figure 7: Buckling mode shape for the composite wing leading-edge panel in axial compression loading.

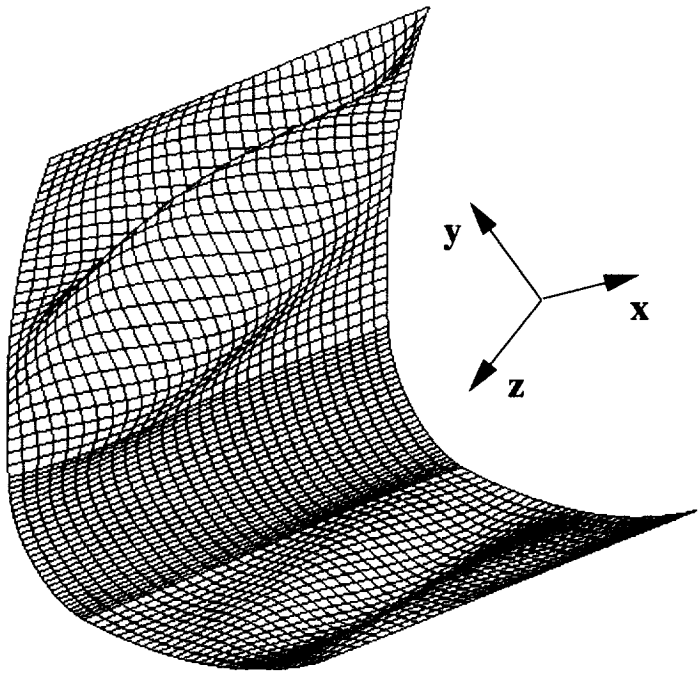


Figure 8: Buckling mode shape for the composite wing leading-edge panel in negative shear loading.

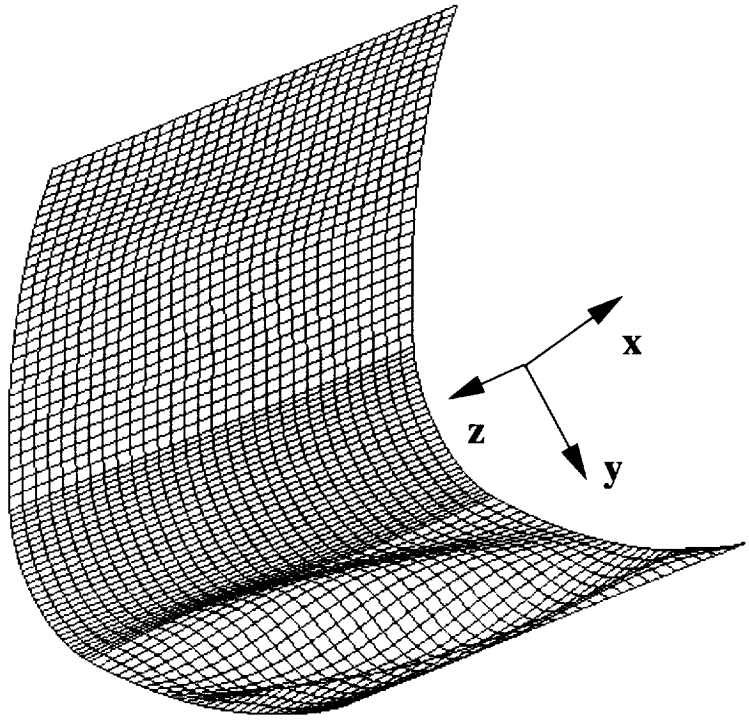


Figure 9: Buckling mode shape for the composite wing leading-edge panel in positive shear loading.